Multigroup Correlated-*k* Distribution Method for Nonequilibrium Atomic Radiation

Ankit Bansal,* M. F. Modest,† and D. A. Levin‡
Pennsylvania State University, University Park, Pennsylvania 16802

Accurate and efficient modeling of shock-layer radiative heat loads is critical for many spacecraft designs. A correlated-*k* distribution method has been developed for the most important atomic species (N and O), which provides great accuracy with high numerical efficiency for the evaluation of radiative transfer in a hot plasma. Challenges posed by typical nonequilibrium gas conditions and extreme concentration and temperature gradients in the shock layer were overcome by splitting the full spectrum into a number of nonoverlapping part spectra. Results for one-dimensional nonhomogeneous gas slabs are presented, comparing line-by-line benchmarks with the full-spectrum correlated-*k* model, showing very good accuracy with a maximum error of 2–3% for the stagnation-line flowfield of the Stardust vehicle and more severe nonhomogeneous two-cell problems.

Nomenclature

a	=	nongray stretching function of k-distributions, dimensionless
b	=	line width, Å
C_2	=	second radiation constant, 1.4388 cm K
c	=	speed of light, 2.9979×10^8 ms^{-1}
f	=	k-distribution, cm
g, g'	=	cumulative k-distribution
h	=	Planck's constant, 6.6262×10^{-34} Js
$I_{b\lambda}$	=	Planck function, W/cm$^2 \cdot$ Å $\cdot$ sr
I_λ	=	intensity, W/cm$^2 \cdot$ Å $\cdot$ sr
k_B	=	Boltzmann constant, $1.3806503 \times 10^{-23}$ m^2 kg s^{-2} K^{-1}
k, k^*	=	reordered absorption coefficient, cm^{-1}
M	=	total number of spectral groups
m	=	atomic mass, kg
N	=	atomic nitrogen
$n, \underline{n}$	=	number density (vector), cm^{-3}
O	=	atomic oxygen
q	=	heat flux, W/cm^2
S	=	atomic line strength, cm^{-1} Å
s	=	space coordinate, cm
T	=	temperature, K
V	=	volume, m^3
w	=	weights of Gaussian quadrature
α	=	transformation parameter for Gauss quadrature
ε_λ	=	spectral emission energy, W/cm$^3 \cdot$ Å $\cdot$ sr
κ_λ	=	absorption coefficient, cm^{-1}
λ	=	wavelength, Å
$\underline{\phi}$	=	gas state vector

Subscripts

b	=	blackbody
cl	=	line center
D	=	Doppler
e	=	electron
g	=	given value of cumulative k-distribution
k	=	given value of reordered absorption coefficient variable
L	=	lower state
m	=	given spectral group
max	=	maximum value of a spectral coefficient
P	=	Planck mean
ref	=	reference conditions
S	=	Stark
U	=	upper state
λ	=	given wavelength
0	=	reference state
1	=	cell 1
2	=	cell 2

Superscripts

bf	=	bound–free
ff	=	free–free
ne	=	nonequilibrium
+	=	ionized species of an atom

*Graduate Student, Department of Mechanical Engineering; azb162@psu.edu.
†Distinguished Professor, Department of Mechanical Engineering; mfm@engr.psu.edu. Fellow AIAA.
‡Professor, Department of Aerospace Engineering; dalevin@psu.edu. Fellow AIAA.

I. Introduction

WHILE entering into the atmosphere of a planet or other planetlike bodies at hypersonic speeds, spacecraft dissipate a large amount of their kinetic energy into heat through shock waves. Accurate computations of the shock-layer radiative heat loads are absolutely necessary for the optimum design of thermal protection systems, because uncertainties of the order of even 20% may have important system design implications. Modeling radiative sources in hypersonic shock layers and fluxes on spacecraft is a highly complex task. Recently, a number of radiative heat-transfer studies have been made, primarily in the context of the Stardust [1–3] and Titan aerocapture missions [4,5], emphasizing the need of accurate predictions of radiative heat loads. NEQAIR96 [6] has been the most widely used code for performing such calculations. NEQAIR96 provides line-by-line (LBL) data of nonequilibrium radiative properties of hypersonic shock-layer plasmas, along with a primitive one-dimensional radiative transport algorithm.

The radiative transfer equation (RTE) is a five-dimensional (three space coordinates and two directions) integro-differential equation and is, consequently, very expensive to solve. To make non-equilibrium shock-layer radiation calculations possible, a number of simplifications have to be made. Most efforts, so far, have been

directed toward solving the RTE with flow solvers in an uncoupled manner. However, the presence of a strong radiation field may significantly alter the population distribution of various radiating species, and a coupled radiative transport solution is desired for a more accurate solution. Absorption coefficients of high-temperature air plasma, as found in the shock layer of spacecraft during atmospheric entry, have very erratic spectral behavior, varying by orders of magnitude over tiny spectral regions. The strong spectral structure of the radiative emission requires a LBL solution of the RTE at several hundred thousand wavelengths, making it prohibitively expensive. Most of the simulations done to date have been limited to simplified quasi-one-dimensional geometries (simple line-of-sight or tangent slab calculations) [7,8]. All these assumptions may lead to very unreliable predictions of radiative heat load onto the spacecraft. Because of the use of the LBL method, coupled solutions with NEQAIR, even for simple one-dimensional geometries, would be prohibitively expensive. More recently, Sohn et al. [9] have developed an efficient databasing scheme that has resulted in a significant reduction of the computation time for spectral coefficients vis-à-vis NEQAIR. Similar to NEQAIR, the database of Sohn et al. uses the quasi-steady-state (QSS) assumption to model nonequilibrium electronic state populations of various energy states. Sohn et al. have demonstrated that their databasing scheme can be applied efficiently to generate spectral coefficients for a given flow condition. However, solving the RTE LBL remains computationally very expensive. It is, therefore, absolutely necessary to develop a spectral radiation model that can predict radiative heating loads in hypersonic shock layers accurately and, at the same time, efficiently by minimizing the number of RTE evaluations.

It has been shown that, for a small spectral interval in a homogeneous medium, the absorption coefficients can be reordered into a monotonic k-distribution, which yields exact results at a fraction of the computational cost required by LBL methods [10,11]. The full-spectrum reordering scheme was first implemented by Denison and Webb [12,13] in the spectral-line-based weighted-sum-of-gray-gases (SLW) model. In this model, detailed spectral absorption coefficient data are used as the basic radiative property to calculate gray-gas weights, rather than experimental data for transmissivity or band absorptance used in the weighted-sum-of-gray-gases (WSGG) model [14,15]. Denison and Webb also extended the SLW model to nonisothermal and nonhomogeneous media. For high-temperature applications Rivière et al. [16] developed the absorption distribution function (ADF) approach, which is almost identical to the SLW model, with the only difference being the evaluation of the gray-gas weights. This method was further generalized by introducing fictitious gases, employing a joint distribution function that separates the gas into two or more fictitious gases and is designed to be more suitable for the treatment of nonhomogeneous media [17]. It was later demonstrated by Modest and Zhang [18] and Modest [19] that the WSGG/SLW/ADF models are step approximations to the smoother full-spectrum k-distribution (FSK) model.

While the k-distribution method is exact for a homogeneous medium, significant errors may occur when applied to strongly nonhomogeneous media. Over the years, a number of new adaptations of the k-distribution method have evolved. The problem of nonhomogeneity is addressed by using one of two different approaches: the scaling approximation or the assumption of a correlated-k distribution [19]. Both the scaled and the correlated-k approaches may result in significant errors when dealing with nonhomogeneous media, because neither the scaled nor the correlated assumptions are ever truly accurate. The resulting errors and the applicability of the full-spectrum scaled-k method and the full-spectrum correlated-k (FSCK) method have been discussed by Modest [19].

It was recognized [20–22] that, in high-temperature combustion applications, with significant temperature changes, totally different spectral lines dominate the radiative transfer, and the assumption of a correlated absorption coefficient breaks down. Similarly, in a mixture of gases, the correlation breaks down in the presence of strong concentration gradients, as recognized by Modest and Zhang [18]. To overcome some of these difficulties, Zhang and Modest

developed the multiscale FSCK distribution method (MSFSCK) [23], where different lines are placed into separate scales based on their temperature dependence, and the multigroup FSCK distribution method [24], where different spectral positions are placed into different spectral groups according to their temperature and pressure dependence. The multigroup model is superior to handle temperature nonhomogeneity within single gas species, while the multiscale model may be better for addressing concentration nonhomogeneity in gas mixtures. The multigroup model has the added advantage that it avoids the problem of overlap between the spectral groups. In contrast, in the MSFSCK method, the approximate treatment of overlap between different scales may lead to additional inaccuracy. A hybrid multiscale multigroup FSK method was developed [25,26] for radiative calculations in a gas mixture containing both temperature and species concentration nonhomogeneities. This method resolves the absorption coefficient of an individual species in a mixture as one of its scales. Within each scale, the wave numbers are placed into exclusive correlated groups.

For high-temperature atomic radiation applications, the reordering concept was first developed by Hermann and Schade [27], in the case of cylindrical nitrogen arcs. This model is very similar to the narrowband-based correlated-k model. The use of the correlated-k method for solving high-temperature shock-layer radiation problems appears very attractive; however, applying it to hypersonic plasmas introduces a number of new difficulties due to thermodynamic nonequilibrium and the presence of a significant number of radiating species. The shock layer of a reentry space vehicle is marked by the presence of extreme temperature and concentration gradients. The nonequilibrium flowfield cannot be represented by a single temperature, and the radiation field is governed by a number of collisional processes. Finally, monatomic species have relatively few spectral lines, but of extreme opacity, making the behavior of line wings of overriding importance. These phenomena make the shock-layer radiation problem very challenging from an FSCK point of view. For the case of atomic radiation, we can take advantage of both the multigroup approach and the multiscale approach. Most of the atomic lines are very narrow and do not overlap with other lines. Also, atomic lines that do overlap have similar temperature and number density dependencies. Thus, atomic lines can be sorted into a number of nonoverlapping spectral groups, with each group also forming a different scale.

In this work, a correlated-k distribution method is developed and applied to the solution of the radiative transfer problem in hypersonic shock layers. The flow in such cases is highly dissociated, and radiation from the atomic species makes, far and away, the most significant contribution [28]. In the present first attempt, we have developed the k-distribution method for the two important radiating species N and O. The model has been tested with the Stardust flowfield. In future work, the method will be extended to include other atomic and diatomic species. The new model will be applied to several Earth and Mars atmospheric entry conditions. However, the model will be developed in such a way that it can be applied to any arbitrary entry conditions on other planetary bodies.

II. Atomic Radiation

In high-temperature nonequilibrium flows, diatomic species may become highly dissociated, and emission from the two atomic species N and O, including bound–bound, bound–free, and free–free transitions, can be the major source of radiation from the shock layer [28]. For atomic radiation, atomic bound–bound lines contribute more to the total radiation than the bound–free and free–free transitions. Atomic lines result from transitions from one electronic state to the other. The QSS model of Park [29] considers a total of 22 energy levels for N and 19 levels for O. Quantum mechanics predicts a number of transitions from one electronic state to the other, leading to emission or absorption of a photon at a specific wavelength. Some electronic transitions are more probable than others; therefore, some lines are stronger than others.

Most atomic lines are optically very thick and have strong self-absorption characteristics. More than 90% of emission from these lines may be absorbed by the line itself over distances as short as 1 mm. Thus, atomic line wings, rather than the line centers, are most important from a heat-transfer point of view. Consequently, it is very important to represent the line shape accurately. Line shape can most realistically be described by the Voigt profile [6,30]. The Voigt profile is defined by Lorentzian and Gaussian line half-widths at half-height. The line width is an important parameter, as it specifies how far from the line center a line retains its strength before its contribution becomes insignificant. Usually, with a Voigt line profile, a strong atomic line may remain important up to 25 to 50 line half-widths on each side of the line, since it is optical thicknesses of order unity that contribute most to the radiative transfer. The Lorentzian width depends on a number of broadening mechanisms. For the case of high-temperature plasmas having high electron number densities, the Lorentz width is essentially governed by Stark broadening, while the Gaussian width comes from Doppler broadening. The Stark width b_S and Doppler width b_D can be written as [31]

$$b_S = 2b_{S,\text{ref}} \left(\frac{T_e}{T_{\text{ref}}}\right)^{0.33} \frac{n_e}{n_{e,\text{ref}}} \qquad (1)$$

$$b_D = \lambda_{\text{cl}} \sqrt{\frac{2k_B T \,\ell n\, 2}{mc^2}} \qquad (2)$$

where $b_{S,\text{ref}}$ is a reference Stark width value at a reference electron temperature of $T_{\text{ref}} = 10,000$ K and a reference electron density of $n_{e,\text{ref}} = 10^{16}$ cm^{-3}; λ_{cl} is the wavelength at the center of an atomic line, and m is the mass of the radiating atom.

In this work, the database developed by Sohn et al. [9] is used to calculate the absorption and emission coefficients for different flow conditions. N has about 170 bound–bound lines, while O has about 86 lines [6,9]. At a resolution of 0.005 Å, it requires, on average, 1000 spectral points to describe a single-line spread over 25–50 line half-widths on each side. This makes the LBL RTE evaluations very expensive, as a total of some quarter-million RTE evaluations will be required.

III. Formulation of Full-Spectrum Correlated-k Method

To understand the various adaptations of FSK methods, it is essential to have a grasp of the basic formulation of the method. In k-distributions, the erratic spectral absorption coefficient is reordered into a monotonically increasing function over a narrow band, part spectrum, or full spectrum. All k-distribution methods to date have been developed for the case of thermodynamic equilibrium, where the radiation field is represented by a single temperature. When the state of a gas in not in thermodynamic equilibrium, it cannot be described by a single temperature. However, the formulation of the k-distribution method for the nonequilibrium case is quite similar, with one major difference being the definition of the Planck function. The RTE for an absorbing and emitting hypersonic plasma can be written as [30]

$$\frac{dI_\lambda}{ds} = \kappa_\lambda(\underline{\phi})[I_{b\lambda}^{ne}(\underline{\phi}) - I_\lambda] \qquad (3)$$

where $\underline{\phi} = (T, T_e, \underline{n})$ is the gas state vector, and $\underline{n}$ is the number density vector specifying concentrations of the species (neutral, ion, and electron). Equation (3) represents transport of energy through an emitting and absorbing medium. Similar to the equilibrium case, the RTE given here is valid for nonequilibrium conditions. However, determination of emission and absorption coefficients for non-equilibrium is subject to some uncertainty [6]. In nonequilibrium, for any given atomic bound–bound transition, the population ratio of upper to lower electronic states, n_L/n_U, replaces the exponential term in the Planck function [6]; that is,

$$I_{b\lambda}(\underline{\phi}) = \frac{2hc^2}{\lambda^5[e^{C_2/\lambda T} - 1]} = \frac{2hc^2}{\lambda^5} \frac{n_U(\underline{\phi})}{n_L(\underline{\phi}) - n_U(\underline{\phi})} \qquad (4)$$

where C_2 is the second radiation constant. Equation (3) is reordered into a k-distribution by multiplying it with the Dirac delta function $\delta[k - \kappa_\lambda(\lambda, \underline{\phi}_0)]$, followed by integration over the entire spectrum. Here, $\kappa_\lambda(\lambda, \underline{\phi}_0)$ is the absorption coefficient evaluated at some reference state $\underline{\phi}_0$. This leads to

$$\frac{dI_k}{ds} = k^*(\underline{\phi}, k)[f(\underline{\phi}, \underline{\phi}_0, k)I_b^{ne}(\underline{\phi}) - I_k] \qquad (5)$$

provided that, at every wavelength across the entire spectrum, where $\kappa_\lambda(\lambda, \underline{\phi}_0) = k$, we must also have a unique value for $\kappa_\lambda(\lambda, \underline{\phi}) = k^*(\underline{\phi}, k)$ everywhere within the medium. In Eq. (5), I_k and f are defined as

$$I_k = \int_0^\infty I_\lambda \delta[k - \kappa_\lambda(\lambda, \underline{\phi}_0)] \, d\lambda \qquad (6)$$

$$f(\underline{\phi}, \underline{\phi}_0, k) = \frac{1}{I_b^{ne}(\underline{\phi})} \int_0^\infty I_{b\lambda}^{ne}(\lambda, \underline{\phi}) \delta[k - \kappa_\lambda(\lambda, \underline{\phi}_0)] \, d\lambda \qquad (7)$$

where $f(\underline{\phi}, \underline{\phi}_0, k)$ is the Planck function-weighted full-spectrum k-distribution, which depends on reference state conditions $\underline{\phi}_0$ through the absorption coefficient and local conditions $\underline{\phi}$ through the non-equilibrium Planck function. Evaluation of an appropriate reference state is a complicated process. A discussion on the evaluation of reference state is given in the next section.

The total intensity I can be obtained by integrating I_k over the reordered k space. The k-distribution can be considered as a probability density function, giving the probability that the absorption coefficient will attain a value k. The k-distribution f has very erratic behavior, and integration in k space is very inconvenient. However, Eq. (5) can be transformed into the much smoother g space by dividing it by the k-distribution at the reference state $f(\underline{\phi}_0, \underline{\phi}_0, k)$, leading to

$$\frac{dI_g}{ds} = k^*(\underline{\phi}_0, \underline{\phi}, g)[a(\underline{\phi}, \underline{\phi}_0, g)I_b^{ne}(\underline{\phi}) - I_g] \qquad (8)$$

with

$$
\begin{aligned}
I_g &= I_k/f(\underline{\phi}_0, \underline{\phi}_0, k) \\
&= \int_0^\infty I_{b\lambda}^{ne}(\lambda, \underline{\phi}) \delta[k - \kappa_\lambda(\lambda, \underline{\phi}_0)] \, d\lambda / f(\underline{\phi}_0, \underline{\phi}_0, k)
\end{aligned} \qquad (9)
$$

where g is the cumulative k-distribution, and $a(\underline{\phi}, \underline{\phi}_0, g)$ is a weight or nongray stretching function given by

$$g(\underline{\phi}_0, \underline{\phi}_0, k) = \int_0^k f(\underline{\phi}_0, \underline{\phi}_0, k) \, dk \qquad (10)$$

$$a(\underline{\phi}, \underline{\phi}_0, g) = \frac{f(\underline{\phi}, \underline{\phi}_0, k)}{f(\underline{\phi}_0, \underline{\phi}_0, k)} = \frac{dg(\underline{\phi}, \underline{\phi}_0, k)/dk}{dg(\underline{\phi}_0, \underline{\phi}_0, k)/dk} \qquad (11)$$

In numerical calculations, it is difficult to evaluate the ratio of the k-distributions f due to their erratic behavior (having singularities at each minimum and maximum of the absorption coefficient [19]); it is much more convenient to evaluate the derivative dg/dk, as indicated in Eq. (11).

Because atomic lines are spread over only a very small part of the spectrum, most of the k-distribution lies in the g range $0.99 \leq g \leq 1$. Thus, for numerical precision reasons, it is preferable to redefine the cumulative k-distribution as

$$g'(\underline{\phi}, k) = 1 - g(\underline{\phi}, k) = \int_k^{k_{\max}} f(\underline{\phi}_0, \underline{\phi}_0, k) \, dk \qquad (12)$$

(i.e., a monotonically decreasing function).

The formulation of the correlated-k method for atomic continuum radiation is exactly the same. Again, the only difference is in the definition of the Planck function that, for continuum radiation, has been defined in terms of spectral emission energy (ε_λ) and absorption coefficient (κ_λ) as

$$I_{b\lambda}^{ne} = \frac{\varepsilon_\lambda^{bf} + \varepsilon_\lambda^{ff}}{\kappa_\lambda^{bf} + \kappa_\lambda^{ff}} \qquad (13)$$

which is consistent with the definition of the Planck function for atomic bound–bound radiation.

IV. Reference State

In principle, the choice of reference state is irrelevant for a truly correlated-k distribution. However, since real k-distributions are not perfectly correlated, the choice of a proper reference state can have significant impact on overall solution accuracy. Since the absorption coefficient is represented exactly only at the reference state (at all other states absorption coefficient is assumed to be correlated to the absorption coefficient at the reference state), an intermediate state is likely to be the most accurate choice for the reference state. For the case of thermodynamic equilibrium, Modest and Zhang [18] have suggested a reference state based on volume-averaged mole fraction and Planck mean temperature based on average emission from the volume. The fact that there is considerable variation in mole fractions from cell to cell, and emission from hot regions often dominates the radiative field, a Planck mean temperature based on overall emitted energy makes a reasonable choice.

For the problem of nonequilibrium atomic radiation, we adopt a similar approach to evaluate the reference state. The radiation process in a hot plasma is dominated by electron collisions. Therefore, the electron temperature is the most important parameter. The Planck function for the nonequilibrium case depends on electron temperature through electronic state population. The electron temperature for the reference state is taken as the Planck mean temperature, based on average emission from the volume. Translation temperature just affects Doppler broadening, and its value for the reference state $\underline{\phi}_0 = (T_0, T_{e0}, \underline{n}_0)$ is chosen as the volume average:

$$\underline{n}_0 = \frac{1}{V} \int_V \underline{n} \, dV \qquad (14)$$

$$T_0 = \frac{1}{V} \int_V T \, dV \qquad (15)$$

$$\kappa_P(\underline{\phi}_0) I_b^{ne}(\underline{\phi}_0) = \frac{1}{V} \int_V \kappa_P(\underline{\phi}) I_b^{ne}(\underline{\phi}) \, dV \qquad (16)$$

where $\kappa_P(\underline{\phi})$ is the Planck mean absorption coefficient and is given by

$$\kappa_P(\underline{\phi}) = \frac{1}{I_b(\underline{\phi})} \int_0^\infty \kappa_\lambda(\underline{\phi}) I_{b\lambda}^{ne}(\underline{\phi}) \, d\lambda \qquad (17)$$

This reference state is labeled ref1 in further discussion. Since the electron temperature is an important parameter in the evaluation of populations of various electronic states, an alternate way to define the reference state would be to take volume-averaged electronic state populations. When the reference state is calculated in this way, reference temperatures can be taken as simple volume-averaged quantities.

$$n_0^e = \frac{1}{V} \int_V n^e \, dV \qquad (18)$$

This reference state will be called ref2 in further discussion.

V. Grouping Scheme for Atomic Lines

The k-distribution method is exact for a homogeneous medium and for truly correlated absorption coefficients. For the case of hypersonic nonequilibrium flow, large temperature and concentration gradients are present within the shock layer and, for such a case, atomic lines appear to not be well correlated. Absorption coefficients of atomic lines and the nonequilibrium Planck function, as defined in Eq. (13), depend on the population of upper and lower electronic states. At higher temperatures, upper states of the atom become more and more populated. Atomic lines resulting from transitions from any of these upper states become stronger in high-temperature regions. The absorption line strength, S, strongly depends on the electron temperature. The dependence of S on electron temperature for N and O is plotted in Figs. 1a and 1b, respectively, for a few selected atomic lines. It can be observed from this figure that different atomic lines have distinct patterns of dependence on electron temperature, each plotted with a different symbol. Lines plotted with the same symbols show similar behavior (lines with square symbols show a continuous gradual decay of S with electron temperature in group 1; lines with delta symbols continuously increase with temperature in group 2; lines with gradient symbols first decrease slightly, then they strongly increase
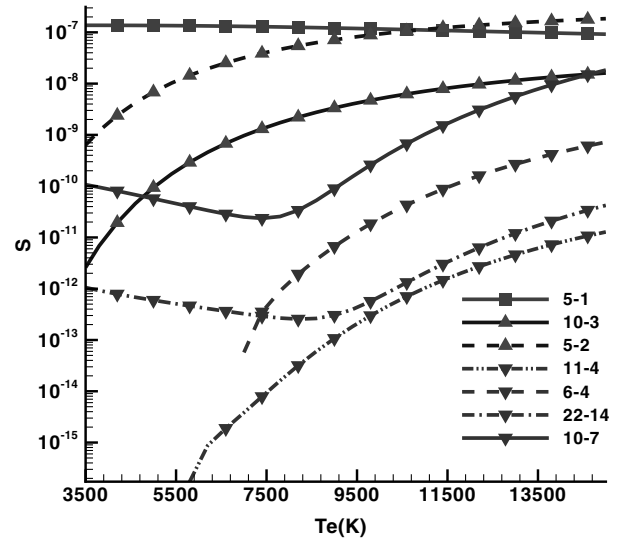
a)
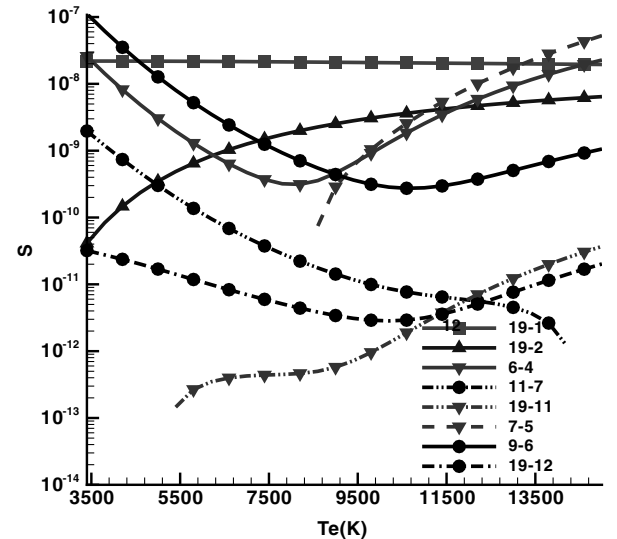
b)

Fig. 1 Dependence of absorption line strength S on electron temperature: a) atomic N and b) atomic O.

with temperature in group 3; finally, lines with circular symbols first decrease with temperature before rising again gradually in group 4). All bound–bound lines of N and O have behaviors similar to one or the other of these selected lines. It was observed that there is very little difference in behavior of atomic N lines between the third and the fourth group. Therefore, for N, these groups were combined into a single group. This dependence is plotted for just one value of neutral, ion, and electron populations. For different values of populations, the dependence is quite similar. The distinct behavior of these atomic lines in different flow conditions results in uncorrelatedness between the k-distributions.

Zhang and Modest [24] have shown that dividing the spectrum into different spectral groups according to their absorption coefficient dependence on gas conditions greatly improves the accuracy of the correlated-k method. We adopt a similar approach for the case of atomic lines. Electronic transitions shown with the same symbols can be combined or put into the same group. After studying results from a large number of heat-transfer studies, it was determined that combining all 170 lines of N into three different nonoverlapping spectral groups and all 86 lines of O into four different spectral groups provides very good accuracy. These spectral groups for N and O are shown in Figs. 2 and 3, respectively. As will be seen, it is also possible to combine similar groups of N and O, provided that separate groups do not overlap with each other. It can be

observed from Fig. 1 that N and O groups, shown in the same symbols, can be combined together. Thus, the total number of groups can be reduced to four, each shown with a different symbol. Also, continuum radiation from both species is modeled as a separate group. Thus, the total spectrum for N and O mixtures can be divided into five groups.
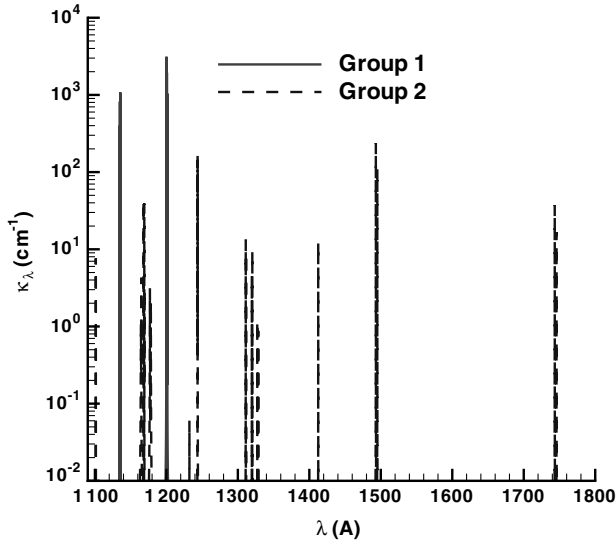
The correlated-k method for the multigroup case can essentially be developed in the same way as for the full spectrum [24]. If we divide the full spectrum into M different part spectra, each containing one group, then for the mth group, multiplying Eq. (3) by the Dirac delta function $\delta[k_m - \kappa_\lambda(\lambda, \underline{\phi}_0)]$, followed by integration across the mth spectral group, leads to

$$\frac{\mathrm{d}I_{km}}{\mathrm{d}s} = k(\underline{\phi}, k_m)[f_m(\underline{\phi}, \underline{\phi}_0, k_m)I_b^{ne}(\underline{\phi}) - I_{k_m}] \qquad (19)$$

where

$$I_{km} = \int_{\lambda \in [\lambda_m]} I_\lambda \delta[k_m - \kappa_\lambda(\lambda, \underline{\phi}_0)]\, \mathrm{d}\lambda \qquad (20)$$

$$f_m(\underline{\phi}, \underline{\phi}_0, k_m) = \frac{1}{I_b^{ne}} \int_{\lambda \in [\lambda_m]} I_{b\lambda}^{ne}(\lambda, \underline{\phi})\delta[k_m - \kappa_\lambda(\lambda, \underline{\phi}_0)]\, \mathrm{d}\lambda \qquad (21)$$
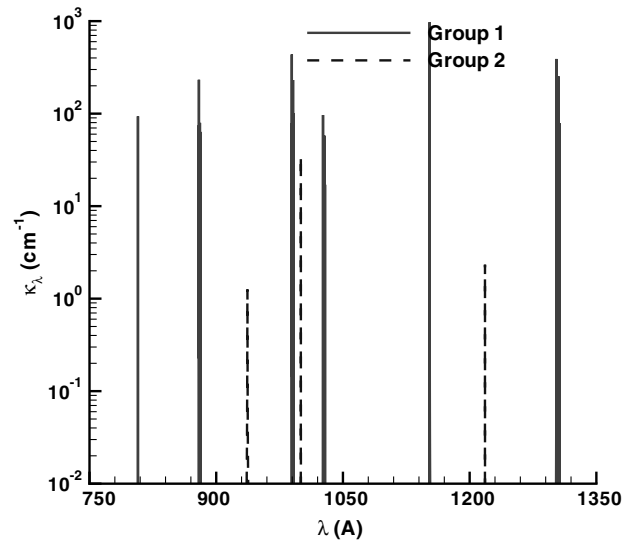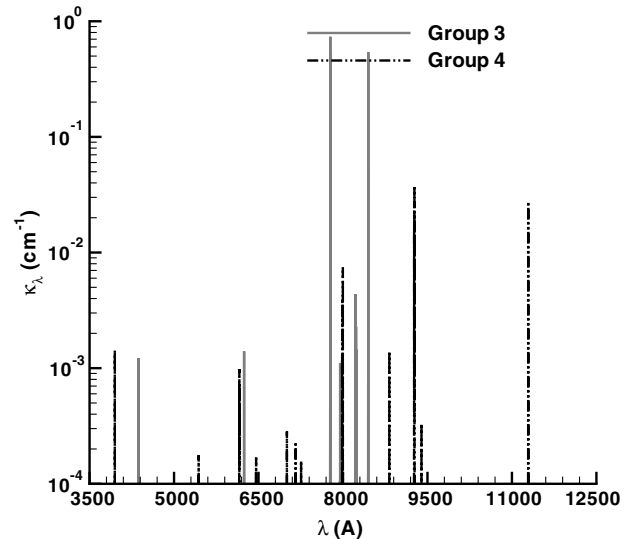

a)
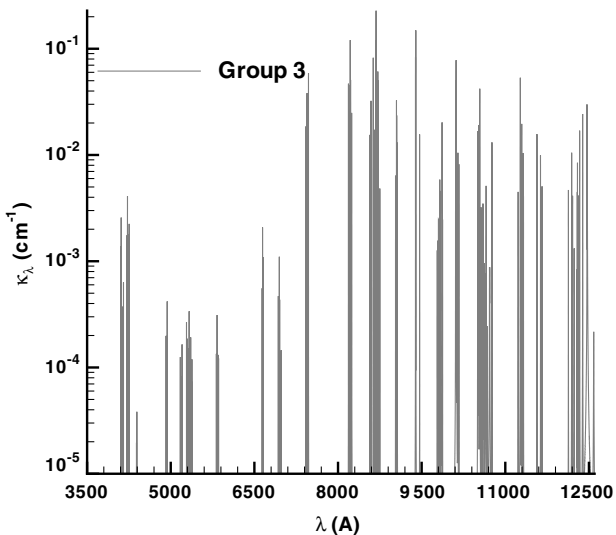
b)

Fig. 2 Spectral groups of atomic lines of N: a) 1100–1800 Å and b) 3500–12500 Å.

a)

b)

Fig. 3 Spectral groups of atomic lines of O: a) 750–1350 Å and b) 3500–12500 Å.

where f is the Planck function-weighted full-spectrum k-distribution for the mth group. Similar to the single-group case, Eq. (19) can be transformed into the much smoother g space, leading to

$$\frac{dI_{gm}}{ds} = k^*(\underline{\phi}_{0,m}, \underline{\phi}, g_m)[a_m(\underline{\phi}, \underline{\phi}_0, g_m)I_b^{ne}(\underline{\phi}) - I_{gm}] \qquad (22)$$

with

$$I_{gm} = I_{km}/f_m(\underline{\phi}_0, \underline{\phi}_0, k_m) \qquad (23)$$

$$g_m(\underline{\phi}_0, \underline{\phi}_0, k_m) = \int_0^{k_m} f_m(\underline{\phi}_0, \underline{\phi}_0, k_m)\, dk_m \qquad (24)$$

$$a(\underline{\phi}, \underline{\phi}_0, g_m) = \frac{f_m(\underline{\phi}, \underline{\phi}_0, k_m)}{f_m(\underline{\phi}_0, \underline{\phi}_0, k_m)} = \frac{dg_m(\underline{\phi}, \underline{\phi}_0, k_m)/dk_m}{dg_m(\underline{\phi}_0, \underline{\phi}_0, k_m)/dk_m} \qquad (25)$$

The total intensity I can be obtained by integrating I_{gm} over the reordered g space and summing over all spectral groups; that is,

$$I = \sum_{m=1}^{M} \int_0^{g_{m,\max}} I_{gm}\, dg_m \qquad (26)$$

$$\sum_{m=1}^{M} g_{m,\max} = 1 \qquad (27)$$

VI. Sample Calculations

To illustrate the validity of the FSCK distribution method to model radiation transfer in hot plasmas containing the atomic species N and O, a few examples are considered. The FSCK method is applied to one-dimensional problems (i.e., solving the RTE using the tangent slab approximation), and the results are compared with those obtained from LBL calculations for the same one-dimensional problems. Since k-distributions just reorder the absorption coefficient, the correlated-k method can be used together with any RTE solver. One-dimensional cases are investigated here for simplicity.

At first, the correlated-k method is applied to a simple two-cell problem. More severe nonhomogeneous conditions of temperatures and gas concentrations are taken than actually present in typical hypersonic shock layers. We will consider two cells bounded by cold black walls. An example for the conditions in the two cells is given in Table 1. These conditions have been appropriately chosen from actual shock-layer conditions. Such two-cell problems with typical conditions serve as an acid test for the method because of its abrupt step change in conditions. In actual applications gradients are much more benign, and the accuracy of the FSCK method can be expected to be better. In this example, radiation from only bound–bound lines is considered. Figures 4a and 4b show the k-distributions for N and O for the conditions given in Table 1. Here, $\underline{\phi}_1$ represents the gas state in cell 1 and $\underline{\phi}_2$ represents the gas state in cell 2. Here, $k(\underline{\phi}_1, \underline{\phi}_2, g_1)$ is the k-distribution for the absorption coefficient at state 2 and the Planck function at state 1. The effect of varying the Planck function on the k-distributions can be understood in terms of the stretching of k in g space. In Fig. 4, this
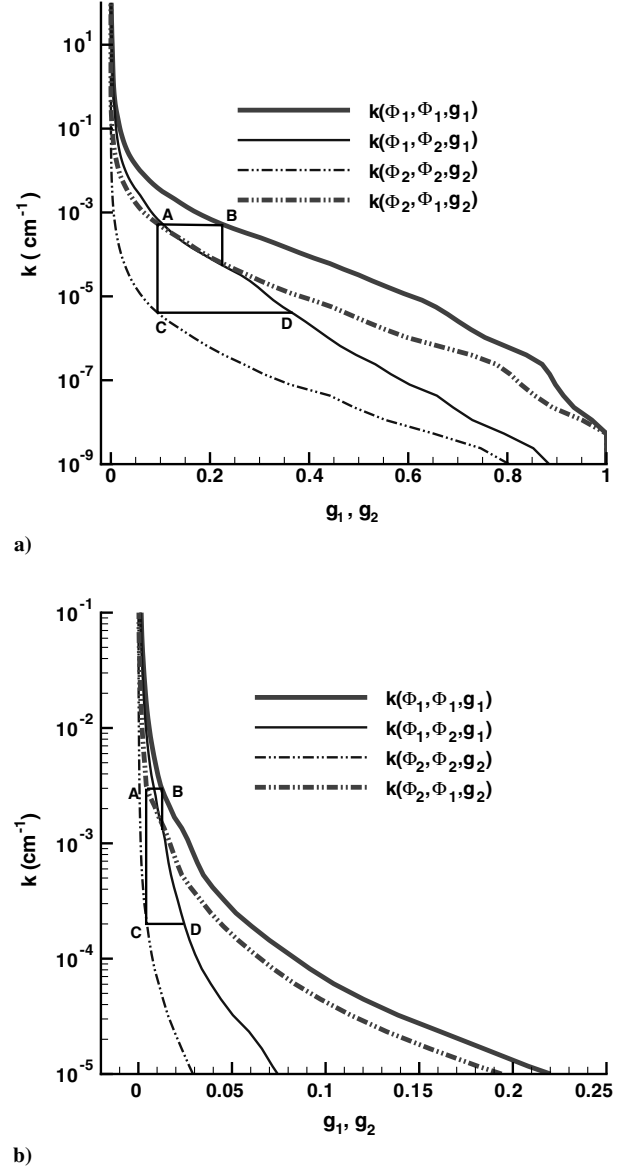

a)

b)

Fig. 4 k-distributions: a) atomic N and b) atomic O.

stretching is represented by lines AB and CD. For exactly correlated-k distributions, the magnitude of stretching in g space would be the same for all flow conditions, and the lines ABCD should form a rectangle. It is clear from this figure that, for such highly nonhomogeneous and nonequilibrium gas conditions, k-distributions are correlated neither for N nor O.

Figure 5 compares the heat flux coming out of the cold cell, as calculated by the LBL and correlated-k methods using different reference states. The problem considers a gas mixture of N and O, with the same properties as given in Table 1. Cell 1 is taken as 1 cm thick while the thickness of cell 2 is varied from 0 to 1.0 cm. It is seen that both reference states based on Planck mean temperature (ref1) and volume-averaged electronic state populations (ref2) provide similar accuracy. Since most radiation is emitted from the hot cell and more than 99% of it gets self-absorbed, even a small error in the prediction of total emission may lead to severe errors. This is the reason that choosing a reference temperature less than the Planck mean temperature leads to large errors, while a temperature greater than the Planck mean gives better results. As the thickness of the cold cell is increased, the reference temperature decreases, leading to larger errors in heat flux. For the multigroup case, the correlation between the absorption coefficients is better than the full-spectrum case; therefore, heat flux results are less sensitive to the choice of the reference state, as shown in Fig. 6. Although a reference temperature

Table 1   Flow conditions for two-cell problem

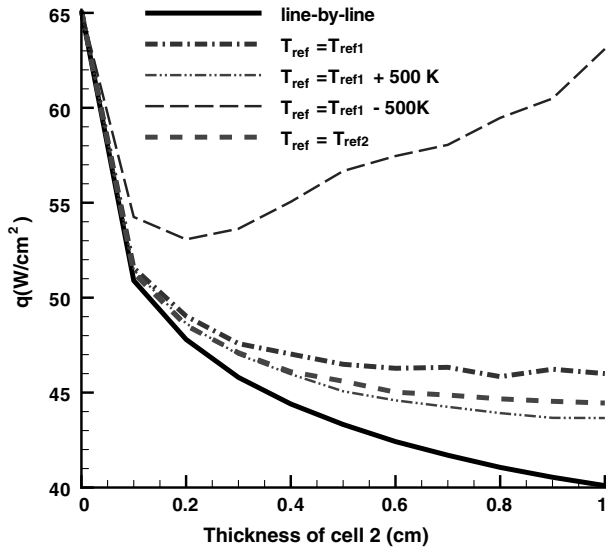|	Cell 1	Cell 2
T, K	24,343	8,578
T_e, K	11,560	8,578
n_N, cm^{-3}	2.7×10^{16}	1.18×10^{17}
n_{N^+}, cm^{-3}	1.2×10^{16}	4.0×10^{15}
n_O, cm^{-3}	1.4×10^{16}	4.9×10^{16}
n_{O^+}, cm^{-3}	3.6×10^{15}	5.5×10^{14}
n_e, cm^{-3}	1.5×10^{16}	4.60×10^{15}

Fig. 5 Full-spectrum cold wall heat flux for varying thickness of cell 2 (ref1 = reference state based on Planck mean, and ref2 = reference state based on volume-averaged electronic state population).
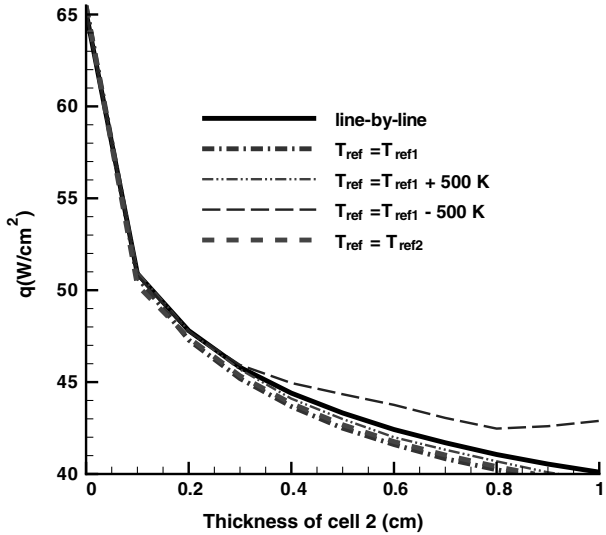

Fig. 6 Multigroup cold wall heat flux for varying thickness of cell 2 (ref1 = reference state based on Planck mean, and ref2 = reference state based on volume-averaged electronic state population).
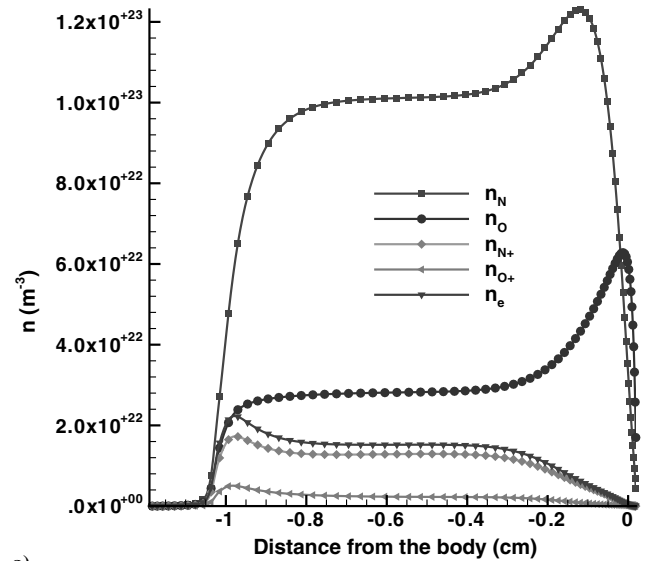
slightly greater than the Planck mean temperature provides the best accuracy, we feel that a reference state based on volume-averaged electronic state population and volume-averaged temperatures provides the best choice for the reference state.

In Table 2, heat fluxes coming out of the cold cell are compared for the same gas state and 1 cm thickness of both cells. Two different cases are considered: 1) a single group for each species and 2) three
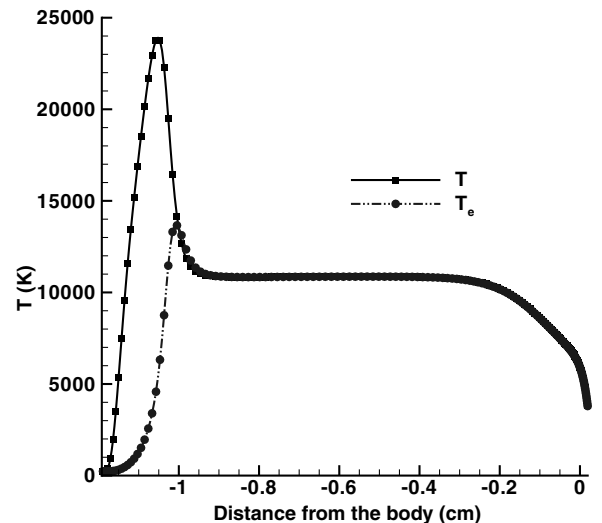
groups for N and four groups for O. It is clear that there is significant improvement in the accuracy of the correlated-k method once atomic lines are grouped according to their absorption characteristics. For both N and O, the error reduces to below 2% for the multigroup case. In the same table, the heat flux results for the mixture of N and O are also compared. The total heat flux from the mixture is found to be almost exactly equal to the sum of the individual gas contributions, indicating that the effect of overlap between N and O lines on heat-transfer results is not significant. As discussed in Sec. V, similar groups of N and O are combined into a total of four groups for the mixture. The error in the heat flux for this case remains below 2%, indicating that the four-group correlated-k method developed in this paper can be applied to gas mixtures of N and O.

In the second example, the peak heating stagnation-line flowfield of the Stardust reentry vehicle is considered. Number densities and temperature profiles for this flowfield are shown in Fig. 7. Again, we will consider the cases of single and multiple groups of lines, and only radiation from bound–bound lines is considered. In Fig. 8, the local heat flux from an N and O mixture along the stagnation line are compared. Reasonable accuracy is obtained when the single-group model is used for the mixture (i.e., the standard FSCK approach), with errors below 5% (compared with the wall flux) except in the unimportant freestream region. Excellent agreement between the

Table 2 Heat flux exiting cold cell, W/cm^2

	LBL	No. of group(s)	Correlated-k	Error
N	31.23	1	34.30	9.83%
N	31.23	3	30.65	1.85%
O	8.86	1	10.21	15.23%
O	8.86	4	8.84	.22%
N + O	40.09	1	44.45	10.87%
N + O	40.09	7	39.44	1.62%
N + O	40.09	4	39.43	1.64%

a)

b)

Fig. 7 Stardust stagnation-line flowfield at peak heating: a) number density plot and b) temperature plot.
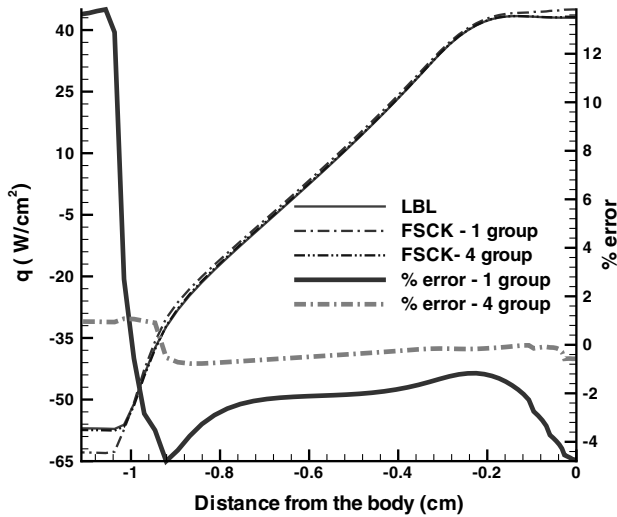
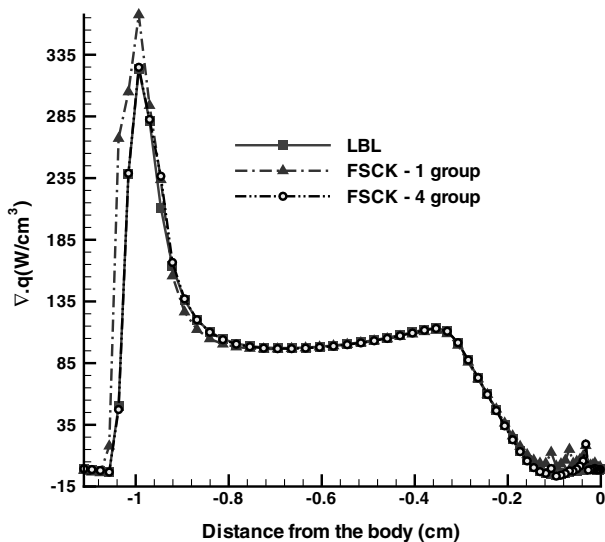**Fig. 8   Heat flux along Stardust stagnation line.**

Fig. 9   Divergence of heat flux along Stardust stagnation line.

LBL and correlated-k results is achieved with the grouping scheme. There is 0.24% error in the radiative heat flux onto the spacecraft for the case of four groups, while the single-group method has an error of 4.20%. The maximum error along the stagnation line is found to be less than 1% for the case of 4 groups, while the single-group approach has a maximum error of about 13% in the freestream region. Similarly, the multigroup k-distribution model provides excellent agreement for divergence of heat flux (radiative heat source) results, as is clear from Fig. 9. It is also clear that the full-spectrum k-distribution method results in larger errors, especially in the shock overshoot region.

Since k-distributions are very smooth, a more efficient integration scheme, such as Gaussian quadrature, can be employed to spectrally integrate the RTE solutions. In the above examples, the RTE was integrated in g space using a 32-point Gauss–Chebyshev quadrature scheme, requiring 32 RTE evaluations (single group) to 128 RTE evaluations (four groups), as opposed to more than 200,000 evaluations required by LBL calculations. The standard Gauss–Chebyshev quadrature scheme puts more quadrature points at higher g values. As already mentioned, it is advantageous to define a monotonically decreasing cumulative k-distribution and, thus, to have more quadrature points at lower g values (i.e., higher k values). This can be achieved by employing a transformation as

$$g'_n = (1 - g_n)^\alpha \qquad (28)$$

A value of $\alpha = 3.0$ places more points at smaller g values and has been used in this work. The modified quadrature weights are given as

$$w'_n = \alpha w_n (1 - g_n)^{\alpha-1} \qquad (29)$$

In future work, we hope to further optimize the quadrature scheme to 8–16 spectral integrations per group. Also, a database of standard k-distributions will be prepared, from which k-distributions for arbitrary flow conditions can be calculated through lookup and interpolation, thus further increasing the efficiency of the k-distribution method.

VII.   Conclusions

The FSCK method was developed for efficient solutions of the RTE in a nonequilibrium flowfield containing N and O species. The accuracy of the FSK method was demonstrated by comparing heat flux results with those obtained from LBL calculations. Reasonable accuracy, with errors below 5% in wall heat flux, was observed for the Stardust stagnation-line flowfield. For more extreme conditions, the FSK method was found to be somewhat less accurate. Atomic lines were separated into a small number of groups according to their absorption characteristics and electronic transitions. The agreement between LBL and multigroup correlated-k results was found to be excellent for different nonhomogeneous two-cell problems. These two-cell problems are taken as extremes representatives of typical nonequilibrium Earth-reentry conditions. The multigroup method developed in this paper is expected to provide great accuracy and efficiency for radiation calculations in Earth's atmosphere. In future work, this method will be applied to the flowfield of the Orion Crew Exploration Vehicle, a bigger spacecraft currently designed by the NASA.

References

[1] Olynick, D., Chen, Y.-K., and Tauber, M. E., "Aerothermodynamics of the Stardust Sample Return Capsule," *Journal of Spacecraft and Rockets*, Vol. 36, No. 3, 1999, pp. 442–462.
doi:10.2514/2.3466

[2] Gupta, R. N., "Aerothermodynamic Analysis of Stardust Sample Return Capsule with Coupled Radiation and Ablation," *Journal of Spacecraft and Rockets*, Vol. 37, No. 4, 2000, pp. 507–514.
doi:10.2514/2.3592

[3] Park, C., "Calculation of Stagnation-Point Heating Rates Associated with Stardust Vehicle," *Journal of Spacecraft and Rockets*, Vol. 44, No. 1, 2007, pp. 24–32.
doi:10.2514/1.15745

[4] Olejniczak, J., Wright, M., Prabhu, D., Takashima, N., Hollis, B., and Zoby, E. V., "An Analysis of the Radiative Heating Environment for Aerocapture at Titan," 39th AIAA/ASME/SAE/ASEE Joint Propulsion Conference and Exhibit, AIAA Paper 2003-4953, 2003.

[5] Wright, M. J., Bose, D., and Olejniczak, J., "The Impact of Flowfield-Radiation Coupling on Aeroheating for Tital Aerocapture," *Journal of Thermophysics and Heat Transfer*, Vol. 19, No. 1, 2005, pp. 17–27.
doi:10.2514/1.10304

[6] Whiting, E., Park, C., Liu, Y., Arnold, J., and Paterson, J., "NEQAIR96, Nonequilibrium and Equilibrium Radiative Transport and Spectra Program: User's Manual," NASA, Publ. 1389, Dec. 1996.

[7] Olynick, D. R., Henline, W. D., Hartung-Chambers, L., and Candler, G. V., "Comparison of Coupled Radiative Flow Solutions with Project Fire 2 Flight Data," *Journal of Thermophysics and Heat Transfer*, Vol. 9, No. 4, 1995, pp. 586–594.
doi:10.2514/3.712

[8] Osawa, H., Matsuyama, S., Ohnishi, N., and Sawada, K., "Comparative Computation of Radiative Heating Environment for Hyugens Probe Entry Flight," 9th AIAA/ASME Joint Thermophysics and Heat Transfer Conference, AIAA Paper 2006-3772, 2006.

[9] Sohn, I., Bansal, A., Levin, D. A., and Modest, M. F., "Advanced Radiation Calculations of Hypersonic Reentry Flows Using Efficient Databasing Schemes," *Journal of Thermophysics and Heat Transfer*, Vol. 24, No. 3, 2010, pp. 623–637.

doi:10.2514/1.45085

[10] Lacis, A. A., and Oinas, V., "A Description of the Correlated-*k* Distribution Method for Modeling Nongray Gaseous Absorption, Thermal Emission, and Multiple Scattering in Vertically Inhomogeneous Atmospheres," *Journal of Geophysical Research*, Vol. 96, No. D5, 1991, pp. 9027–9063.
doi:10.1029/90JD01945

[11] Goody, R. M., and Yung, Y. L., *Atmospheric Radiation—Theoretical Basis*, 2nd ed., Oxford University Press, New York, 1989.

[12] Denison, M. K., and Webb, B. W., "A Spectral Line Based Weighted-Sum-of-Gray-Gases Model for Arbitrary RTE Solvers," *Journal of Heat Transfer*, Vol. 115, No. 4, 1993, pp. 1004–1012.
doi:10.1115/1.2911354

[13] Denison, M. K., and Webb, B. W., "The Spectral-Line-Based Weighted-Sum-of-Gray-Gases Model in Nonisothermal Nonhomogeneous Media," *Journal of Heat Transfer*, Vol. 117, No. 2, 1995, pp. 359–365.
doi:10.1115/1.2822530

[14] Hottel, H. C., and Sarofim, A. F., *Radiative Transfer*, McGraw–Hill, New York, 1967.

[15] Modest, M. F., "The Weighted-Sum-of-Gray-Gases Model for Arbitrary Solution Methods in Radiative Transfer," *Journal of Heat Transfer*, Vol. 113, No. 3, 1991, pp. 650–656.
doi:10.1115/1.2910614

[16] Rivière, P., Soufiani, A., Perrin, M. Y., Riad, H., and Gleizes, A., "Air Mixture Radiative Property Modelling in the Temperature Range 10,000–40,000 K," *Journal of Quantitative Spectroscopy and Radiative Transfer*, Vol. 56, No. 1, 1996, pp. 29–45.
doi:10.1016/0022-4073(96)00033-7

[17] Pierrot, L., Rivière, P., Soufiani, A., and Taine, J., "A Fictitious-Gas-Based Absorption Distribution Function Global Model for Radiative Transfer in Hot Gases," *Journal of Quantitative Spectroscopy and Radiative Transfer*, Vol. 62, No. 5, 1999, pp. 609–624.
doi:10.1016/S0022-4073(98)00124-1

[18] Modest, M. F., and Zhang, H., "The Full-Spectrum Correlated-*k* Distribution For Thermal Radiation from Molecular Gas–Particulate Mixtures," *Journal of Heat Transfer*, Vol. 124, No. 1, 2002, pp. 30–38.
doi:10.1115/1.1418697

[19] Modest, M. F., "Narrow-Band and Full-Spectrum *k*-Distributions for Radiative Heat Transfer: Correlated-*k* vs. Scaling Approximation," *Journal of Quantitative Spectroscopy and Radiative Transfer*, Vol. 76, No. 1, 2003, pp. 69–83.
doi:10.1016/S0022-4073(02)00046-8

[20] Rivière, P., Soufiani, A., and Taine, J., "Correlated-*k* and Fictitious Gas Methods for H_2O Near 2.7 μm," *Journal of Quantitative Spectroscopy and Radiative Transfer*, Vol. 48, No. 2, 1992, pp. 187–203.

doi:10.1016/0022-4073(92)90088-L

[21] Rivière, P., Soufiani, A., and Taine, J., "Correlated-*k* and Fictitious Gas Model for H_2O Infrared Radiation in the Voigt Regime," *Journal of Quantitative Spectroscopy and Radiative Transfer*, Vol. 53, No. 3, 1995, pp. 335–346.
doi:10.1016/0022-4073(94)00122-N

[22] Rivière, P., Scutaru, D., Soufiani, A., and Taine, J., "A New $c - k$ Data Base Suitable from 300 to 2500 K for Spectrally Correlated Radiative Transfer in CO_2-H_2O Transparent Gas Mixtures," *Tenth International Heat Transfer Conference*, Taylor and Francis, Washington, D.C., 1994, pp. 129–134.

[23] Zhang, H., and Modest, M. F., "A Multi-Scale Full-Spectrum Correlated-*k* Distribution for Radiative Heat Transfer in Inhomogeneous Gas Mixtures," *Journal of Quantitative Spectroscopy and Radiative Transfer*, Vol. 73, Nos. 2–5, 2002, pp. 349–360.
doi:10.1016/S0022-4073(01)00220-5

[24] Zhang, H., and Modest, M. F., "Scalable Multi-Group Full-Spectrum Correlated-*k* Distributions for Radiative Heat Transfer," *Journal of Heat Transfer*, Vol. 125, No. 3, 2003, pp. 454–461.
doi:10.1115/1.1560156

[25] Wang, L., and Modest, M. F., "A Hybrid Multi-Scale Full-Spectrum *k*-Distribution Method for Radiative Transfer in Inhomogeneous Gas Mixtures," *Proceedings of IMECE 2005*, American Society of Mechanical Engineers, New York, 2005, pp. 175–182.

[26] Pal, G., Modest, M. F., and Wang, L., "Hybrid Full-Spectrum Correlated *k*-Distribution Method for Radiative Transfer in Nonhomogeneous Gas Mixtures," *Journal of Heat Transfer*, Vol. 130, No. 8, 2008, Paper 082701.
doi:10.1115/1.2909612

[27] Hermann, W., and Schade, E., "Radiative Energy Balance in Cylindrical Nitrogen Arcs," *Journal of Quantitative Spectroscopy and Radiative Transfer*, Vol. 12, No. 9, 1972, pp. 1257–1282.
doi:10.1016/0022-4073(72)90183-5

[28] Bose, D., McCorkle, E., Thompson, E., Bogdanoff, D., Prabhu, D. K., Allen, G. A., and Grinstead, J., "Analysis and Model Validation of Shock Layer Radiation in Air," 46th AIAA Aerospace Sciences Meeting and Exhibit, AIAA Paper 2008-1246, 2008.

[29] Park, C., *Nonequilibrium Hypersonic Aerothermodynamics*, Wiley, New York, 1990.

[30] Modest, M. F., *Radiative Heat Transfer*, 2nd ed., Academic Press, New York, 2003.

[31] Hartung-Chambers, L., "Predicting Radiative Heat Transfer in Thermochemical Nonequilibrium Flow Fields," NASA TM 4564, 1994.